Exact Expression for the Lifting Condensation Level

David M. Romps

Department of Earth and Planetary Science, University of California, Berkeley, and Climate and Ecosystem Sciences Division, Lawrence Berkeley National Laboratory, Berkeley, California

Abstract

Many analytic, but approximate, expressions have been proposed for the height of the lifting condensation level (LCL), including the popular expressions by Espy, Bolton, and Lawrence. Here, the exact, explicit, analytic expression is derived for an air parcel's LCL as a function of its temperature and relative humidity. Unlike previous analytic expressions, some of which can have errors as high as hundreds or thousands of meters, this exact expression is accurate to within the uncertainty of empirical vapor pressure measurements: this translates into an uncertainty of around 5 m for all temperatures and relative humidities. An exact, explicit, analytic expression for the lifting deposition level (LDL) is also derived, and its behavior is compared to the LCL. At sufficiently cold temperatures, aerosols freeze homogeneously below the LCL; an approximate, implicit, analytic expression is given for this lifting freezing level (LFL). By comparing the LCL, LDL, and LFL, it is found that a well-mixed boundary layer can have an ice-supersaturated layer that is no thicker than 400 m.

Keywords: Cloud cover; Clouds; Condensation; Cumulus clouds

Corresponding author: David M. Romps, romps@berkeley.edu

1. Introduction

The lifting condensation level (LCL) is the height at which an air parcel would saturate if lifted adiabatically. The LCL is a key concept in the prediction of cloud cover (e.g., Wetzel 1990), the parameterization of convection and precipitation in weather and climate models (e.g., Emanuel and Živković-Rothman 1999), and the interpretation of atmospheric dynamics on other planets (e.g., Atreya et al. 2006). Over the past 180 years, many explicit, analytic expressions have been proposed to approximate the LCL as a function of temperature and humidity, but none of those expressions is exact, and none of them is expressed in terms of fundamental physical constants.

The first equation for the LCL was given by Espy (1836, p. 244), who wrote that, as soon as the ascending air was "as many hundred yards high as the temperature of the air on the ground was above the dew-point in degrees of Fahrenheit, the cold produced by the expansion of the air would begin to condense the vapour and form clouds." Since 1 yd equals 0.9144 m and 1°F equals (5/9)°C, this means that the LCL is given by $z_{\rm LCL} = z + (100\,\text{yards}\,^\circ\text{F}^{-1})(T - T_d) = z + (165\,\text{m}\,\text{K}^{-1})(T - T_d)$, where z, T, and T_d

are the parcel's initial height, temperature, and dewpoint temperature, respectively. Subsequent studies established that the coefficient should be closer to 137 m K^{-1} (Davis 1889), and the coefficient was later revised down to 123 m K^{-1} (McDonald 1963). Most recently, it has been suggested by Lawrence (2005) that the optimal value is 125 m K^{-1}, giving

$$z_{\mathrm{LCL}} = z + (125\,\mathrm{m\,K^{-1}})(T - T_d) \quad \text{(Espy)}. \qquad (1)$$

In the years since Espy's original work, more complicated formulas were proposed, including the oft-used Eq. (22) of Bolton (1980) for the temperature of the LCL, which we can convert to a height as

$$z_{\mathrm{LCL}} = z + \frac{c_{pm}}{g}\left\{T - 55\,\mathrm{K} - \left[\frac{1}{T - 55\,\mathrm{K}} - \frac{\log(\mathrm{RH}_l)}{2840\,\mathrm{K}}\right]^{-1}\right\}, \qquad (2)$$

where z is the parcel's height, T is its absolute temperature, K denotes units of kelvins, RH_l is the parcel's relative humidity with respect to liquid, which ranges from 0 to 1, and c_{pm}/g is the inverse of the dry adiabatic lapse rate with $g = 9.81$ m s^{-2} the gravitational acceleration and c_{pm} the parcel's heat capacity at constant pressure (a precise definition of c_{pm} is given in section 3). Bolton (1980) also gives an implicit expression for the LCL in his Eq. (18), but that equation is not analytic; it must be solved using a numerical root solver. Finally, more recently, Lawrence (2005) proposed a formula of intermediate complexity, which is

$$z_{\mathrm{LCL}} = z + \left(20 + \frac{T - 273.15\,\mathrm{K}}{5\,\mathrm{K}}\right)(100\,\mathrm{m})(1 - \mathrm{RH}_l), \quad (3)$$

where z is the parcel's height, T is its absolute temperature, K denotes units of kelvins, m denotes units of meters, and RH_l ranges from 0 to 1. The intention of Lawrence (2005) is for this expression to be applied to parcels with $0.5 \le \mathrm{RH}_l \le 1$ and $273 < T < 303\,\mathrm{K}$.

The present study eliminates the need for this proliferation of formulas by deriving an exact, explicit, analytic expression for the LCL in the context of constant heat capacities. The tiny errors introduced by assuming constant heat capacities are also quantified: the uncertainty in this exact expression is less than or equal to about 5 m. For those eager to use the exact expression for the LCL, it may be found in Eq. (22). The analogous equation for the lifting deposition level (LDL) may be found in Eq. (23). These functions are available for download from the author's website in a variety of programming languages (currently R, Python, Fortran, and MATLAB).

2. Constant heat capacities

To derive an exact, explicit, analytic expression for the LCL, we will need to use constant values for the heat capacities of water. Although heat capacities do vary somewhat with temperature, neglecting this variation is standard practice. In this section, we show that a careful choice of gas

constant and heat capacities can put the analytic expressions for saturation vapor pressure into excellent agreement with laboratory measurements. The reader who is comfortable with the use of constant heat capacities may skip to the next section.

Let $p_v^{*,l}(T)$ be the saturation vapor pressure of liquid water at temperature T. For an arbitrary temperature T, and assuming constant heat capacities, $p_v^{*,l}(T)$ is given by (Romps 2008; Romps and Kuang 2010; Romps 2015)

$$p_v^{*,l} = p_{\text{trip}} \left(\frac{T}{T_{\text{trip}}} \right)^{(c_{pv}-c_{vl})/R_v} \times \exp\left[\frac{E_{0v} - (c_{vv}-c_{vl})T_{\text{trip}}}{R_v} \left(\frac{1}{T_{\text{trip}}} - \frac{1}{T} \right) \right], \quad (4)$$

where R_v is the specific gas constant for water vapor, c_{vv} is the specific heat capacity of water vapor at constant volume, $c_{pv} = c_{vv} + R_v$ is the specific heat capacity of water vapor at constant pressure, c_{vl} is the specific heat capacity of liquid water, p_{trip} is the triple-point vapor pressure, T_{trip} is the triple-point temperature, and E_{0v} is the difference in specific internal energy between water vapor and liquid at the triple point. Similarly, defining $p_v^{*,s}(T)$ to be the saturation vapor pressure of solid water (i.e., ice) at temperature T, $p_v^{*,s}(T)$ is given by

$$p_v^{*,s} = p_{\text{trip}} \left(\frac{T}{T_{\text{trip}}} \right)^{(c_{pv}-c_{vs})/R_v} \times \exp\left[\frac{E_{0v} + E_{0s} - (c_{vv}-c_{vs})T_{\text{trip}}}{R_v} \left(\frac{1}{T_{\text{trip}}} - \frac{1}{T} \right) \right], \quad (5)$$

where c_{vs} is the specific heat capacity of solid water and E_{0s} is the difference in specific internal energy between liquid and solid at the triple point. The values of c_{vv}, p_{trip}, T_{trip}, E_{0v}, and E_{0s} used here are

$$c_{vv} = 1418\,\text{J kg}^{-1}\,\text{K}^{-1}, \quad (6)$$

$$p_{\text{trip}} = 611.65\,\text{Pa}, \quad (7)$$

$$T_{\text{trip}} = 273.16\,\text{K}, \quad (8)$$

$$E_{0v} = 2.3740 \times 10^6\,\text{J kg}^{-1}, \quad (9)$$

$$E_{0s} = 0.3337 \times 10^6\,\text{J kg}^{-1}. \quad (10)$$

Rather than specify the values of R_v, c_{vl}, and c_{vs} a priori, we will choose their values to minimize the fractional difference between the saturation vapor

pressures given in Eqs. (4) and (5) and the saturation vapor pressures given by Wagner and Pruß (2002) and Wagner et al. (2011) based on laboratory data. Allowing those three parameters to vary, the optimization method of Nelder and Mead (1965) is used to minimize the following objective function:

$$\frac{1}{273\,\mathrm{K}-180\,\mathrm{K}}\int_{180\,\mathrm{K}}^{273\,\mathrm{K}} dT\left[\frac{p_v^{*,s}(T)}{p_v^{*,s,\mathrm{Wagner}}(T)}-1\right]^2 + \frac{1}{330\,\mathrm{K}-230\,\mathrm{K}}\int_{230\,\mathrm{K}}^{330\,\mathrm{K}} dT\left[\frac{p_v^{*,l}(T)}{p_v^{*,l,\mathrm{Wagner}}(T)}-1\right]^2.$$

This identifies the optimal values, which are

$$R_v = 461\,\mathrm{J\,kg^{-1}\,K^{-1}}, \tag{11}$$

$$c_{vl} = 4119\,\mathrm{J\,kg^{-1}\,K^{-1}}, \tag{12}$$

$$c_{vs} = 1861\,\mathrm{J\,kg^{-1}\,K^{-1}}. \tag{13}$$

Figure 1a compares $p_v^{*,s}$ from Eq. (5) with the ice-saturation expressions given by Sonntag (1990), Murphy and Koop (2005), and Wagner et al. (2011), which are fits to laboratory data; see the appendix for the formulas. Each of these four expressions is plotted as the fractional deviation (%) from the average of all four. Also included are the recent laboratory measurements of Bielska et al. (2013), plotted as circles with error bars; these are also plotted as the fractional deviation from the mean of the four expressions. As is evident, all of these expressions and data agree with each other to within ±1% over the full range of temperature from 180 to 273 K.

Figure 1b compares the $p_v^{*,l}$ from Eq. (4) with the liquid-saturation expressions given by Sonntag and Heinze (1982), Murphy and Koop (2005), and Wagner and Pruß (2002), which are also fits to laboratory data; see the appendix for the formulas. Here, the agreement is better than ±0.5% over the full range of temperature from 233 to 330 K. This agreement is not guaranteed for other choices of R_v, c_{vl}, and c_{vs}. For example, if we were to use a value of c_{vs} = 2106 J kg^{-1} K^{-1}, which is listed in many textbooks (e.g., Riegel 1992; Tsonis 2002; Wallace and Hobbs 2006; Cotton et al. 2011; Brasseur and Jacob 2017), we would get a $p_v^{*,s}$ that deviates from empirical measurements by several percent at a temperature of 180 K.

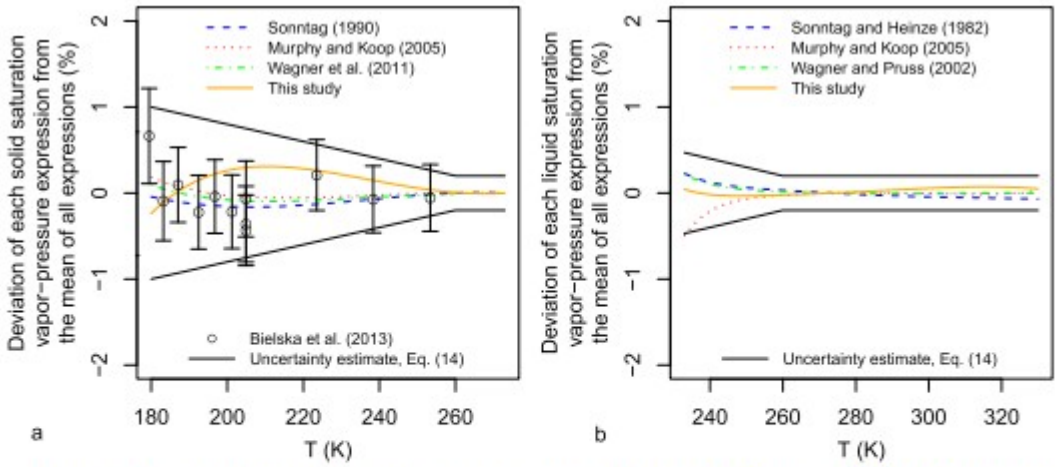

FIG. 1. (a) The saturation vapor pressure over ice as represented by Eq. (A1) (from Sonntag 1990) (dashed blue), Eq. (A2) (from Murphy and Koop 2005) (dotted red), Eq. (A3) (from Wagner et al. 2011) (dash–dotted green), and Eq. (5) (solid orange), all plotted as their fractional deviation (%) from the average of all four. The circles and associated error bars come from the laboratory measurements of Bielska et al. (2013). The solid black curves plot the estimated upper bound on the uncertainty from Eq. (14). (b) As in (a), but for the saturation vapor pressure over liquid as represented by Eq. (A4) (from Sonntag and Heinze 1982) (dashed blue), Eq. (A5) (from Murphy and Koop 2005) (dotted red), Eq. (A6) (from Wagner and Pruß 2002) (dash–dotted green), and Eq. (4) (solid orange).

From Fig. 1, we conclude that the values in Eqs. (6)–(13) do an excellent job of replicating the thermodynamics of water from 180 to 330 K. To quantify the remaining error or uncertainty, we can construct a simple function $U(T)$ such that $\pm U$ bounds the expressions and data in Fig. 1. The fractional uncertainty U is modeled as

$$U = \begin{cases} 0.002 & T \geq 260\,\mathrm{K} \\ 0.01 + (0.002 - 0.01)\dfrac{T - 180\,\mathrm{K}}{260\,\mathrm{K} - 180\,\mathrm{K}} & T < 260\,\mathrm{K} \end{cases}, \tag{14}$$

and $+U$ and $-U$ are plotted in Fig. 1 as the solid black lines. Note that the difference between the vapor pressures derived here and the expressions from the other studies is comparable to the differences among the expressions from the other studies. Therefore, U can be thought of as both an upper bound on the uncertainty (i.e., the empirical uncertainty as to the true saturation vapor pressure) and an upper bound on the error (i.e., the deviation from the true vapor pressure caused by using analytical vapor pressure expressions with constant heat capacities).

3. Exact expression

In this section, we will derive an exact expression for an air parcel's LCL height using the analytic saturation vapor pressures. Let us denote the air parcel's initial pressure and temperature by p and T, respectively. Let us also denote the air parcel's pressure and temperature at its LCL by p_{LCL} and T_{LCL}, respectively. As a parcel of air is transported adiabatically to its LCL, its potential temperature is exactly conserved, which allows us to relate its LCL

pressure and temperature (p_{LCL} and T_{LCL}) to its initial pressure and temperature (p and T) by

$$p_{\mathrm{LCL}} = p\left(\frac{T_{\mathrm{LCL}}}{T}\right)^{c_{pm}/R_m}, \tag{15}$$

where R_m is the air parcel's specific gas constant and c_{pm} is its specific heat capacity at constant pressure. The subscript m denotes that these are the appropriate values for moist air, that is,

$$R_m = (1 - q_v)R_a + q_v R_v, \tag{16}$$

$$c_{pm} = (1 - q_v)c_{pa} + q_v c_{pv}, \tag{17}$$

where q_v is the mass fraction of water vapor, R_a is the specific gas constant of dry air, $c_{pa} = c_{va} + R_a$ is the specific heat capacity at constant pressure for dry air, and R_v and c_{pv} are as defined in section 2. The values used for R_a and c_{va} are

$$R_a = 287.04\,\mathrm{J\,kg^{-1}\,K^{-1}}, \tag{18}$$

$$c_{va} = 719\,\mathrm{J\,kg^{-1}\,K^{-1}}. \tag{19}$$

By the ideal gas law, the partial pressure of water vapor p_v and the total pressure p are related by $p_v = (R_v q_v / R_m)p$. Adiabatic lifting of a parcel from its initial p to p_{LCL} does not change its q_v, and therefore, $R_v q_v / R_m$ is the same at pressures p and p_{LCL}. Therefore, we can multiply the left-hand and right-hand sides of Eq. (15) by the unique value of $R_v q_v / R_m$ to get

$$p_{v,\mathrm{LCL}} = p_v\left(\frac{T_{\mathrm{LCL}}}{T}\right)^{c_{pm}/R_m}. \tag{20}$$

This relates a parcel's vapor pressure $p_{v,\mathrm{LCL}}$ at its LCL to its initial vapor pressure p_v and temperature T.

Next, we can use Eq. (4) to relate the parcel's saturation vapor pressure with respect to liquid at its LCL temperature $p_v^{*,l}(T_{\mathrm{LCL}})$ to its saturation vapor pressure with respect to liquid at its initial temperature $p_v^{*,l}(T)$. This yields

$$p_v^{*,l}(T_{\mathrm{LCL}}) = p_v^{*,l}(T)\left(\frac{T_{\mathrm{LCL}}}{T}\right)^{(c_{pv}-c_{vl})/R_v} \times \exp\left[\frac{E_{0v} - (c_{vv} - c_{vl})T_{\mathrm{trip}}}{R_v T}\left(1 - \frac{T}{T_{\mathrm{LCL}}}\right)\right]. \tag{21}$$

The next step is to recognize that $p_{v,\mathrm{LCL}} = p_v^{*,l}(T_{\mathrm{LCL}})$, so the left-hand sides of Eqs. (20) and (21) are equal. Dividing Eq. (20) by Eq. (21), we get

$$1 = \mathrm{RH}_l \left(\frac{T_{\mathrm{LCL}}}{T}\right)^{c_{pm}/R_m - (c_{pv}-c_{vl})/R_v} \times \exp\left[-\frac{E_{0v} - (c_{vv}-c_{vl})T_{\mathrm{trip}}}{R_v T}\left(1 - \frac{T}{T_{\mathrm{LCL}}}\right)\right],$$

where $\mathrm{RH}_l = p_v/p_v^{*,l}$ is the air parcel's initial relative humidity with respect to liquid. Defining $x = T/T_{\mathrm{LCL}}$, this equation is of the form $1 = \mathrm{RH}_l x^{-a} e^{b(1-x)}$, where a, b, and RH_l are all independent of T_{LCL}: they depend only on fundamental parameters and the initial properties of the air parcel. Taking this equation to the power $1/a$ and defining $c = b/a$, we can then rearrange the equation to get

$$cxe^{cx} = \mathrm{RH}_l^{1/a} c e^{c}.$$

This can be solved using the Lambert W function, which is defined by $W(ye^y) = y$. The Lambert W function is double valued when its argument is negative; since $c < 0$ and $x \geq 1$, we want the -1 branch, which is denoted by W_{-1}. Taking W_{-1} of the above equation, we get

$$cx = W_{-1}(\mathrm{RH}_l^{1/a} c e^{c}).$$

In a boundary layer with a dry adiabatic lapse rate, the dry static energy of a lifted parcel will be conserved, implying that the height above the ground at which the parcel's temperature equals T_{LCL} will be $z_{\mathrm{LCL}} = z + c_{pm}(T - T_{\mathrm{LCL}})/g$. In fact, the parcel's dry static energy will be very nearly conserved even in a boundary layer without a dry adiabatic lapse rate because the change in dry static energy for an adiabatically lifted parcel is proportional to its buoyancy (Romps 2015), and the typical buoyancy of parcels in a boundary layer is small. Therefore, the LCL temperature T_{LCL}, the LCL pressure p_{LCL}, and the LCL height z_{LCL} are

$$T_{\mathrm{LCL}} = c[W_{-1}(\mathrm{RH}_l^{1/a} c e^{c})]^{-1} T, \tag{22a}$$

$$p_{\mathrm{LCL}} = p\left(\frac{T_{\mathrm{LCL}}}{T}\right)^{c_{pm}/R_m}, \tag{22b}$$

$$z_{\mathrm{LCL}} = z + \frac{c_{pm}}{g}(T - T_{\mathrm{LCL}}), \tag{22c}$$

$$a = \frac{c_{pm}}{R_m} + \frac{c_{vl} - c_{pv}}{R_v}, \tag{22d}$$

$$b = -\frac{E_{0v} - (c_{vv} - c_{vl})T_{\mathrm{trip}}}{R_v T}, \tag{22e}$$

$$c = b/a. \tag{22f}$$

These equations give the parcel's pressure, temperature, and height at its LCL (p_{LCL}, T_{LCL}, and z_{LCL}) in terms of its initial pressure, temperature, and

height (p, T, and z). Since W is a well-known special function, these are analytic expressions for the properties of the LCL. Equations (22a) and (22b) give the exact temperature and pressure of the parcel when it reaches saturation through adiabatic expansion. If that adiabatic expansion takes place in a well-mixed layer, then Eq. (22c) gives the exact height to which the parcel must ascend to saturate. We can easily check the limiting behaviors of Eq. (22a). When $\mathrm{RH}_l = 1$, we can use the fact that $W_{-1}(ce^c) = c$ to confirm that $T_{\mathrm{LCL}} = T$. As $\mathrm{RH}_l \to 0$, we can use the fact that $W_{-1}(x) \to -\log(-x)$ as $|x| \to 0$ to confirm that $T_{\mathrm{LCL}} \to 0$. For a well-mixed layer, this would imply that the well-mixed subcloud layer occupies the entire atmosphere up to an altitude of $c_{pa}T/g$. Note that Eq. (22) describes the pressure, temperature, and altitude of the lifting *condensation* level (i.e., the height at which the parcel's vapor pressure equals the saturation vapor pressure over liquid water).

Similarly, we can define the lifting *deposition* level (LDL) as the height at which the parcel's vapor pressure equals the saturation vapor pressure over solid water (i.e., ice). Above the LDL, the air parcel may form ice by heterogeneous deposition nucleation. Proceeding as in the derivation of the LCL, the LDL is found to be

$$T_{\mathrm{LDL}} = c[W_{-1}(\mathrm{RH}_s^{1/a} ce^c)]^{-1} T, \tag{23a}$$

$$p_{\mathrm{LDL}} = p\left(\frac{T_{\mathrm{LDL}}}{T}\right)^{c_{pm}/R_m}, \tag{23b}$$

$$z_{\mathrm{LDL}} = z + \frac{c_{pm}}{g}(T - T_{\mathrm{LDL}}), \tag{23c}$$

$$a = \frac{c_{pm}}{R_m} + \frac{c_{vs} - c_{pv}}{R_v}, \tag{23d}$$

$$b = -\frac{E_{0v} + E_{0s} - (c_{vv} - c_{vs})T_{\mathrm{trip}}}{R_v T}, \tag{23e}$$

$$c = b/a. \tag{23f}$$

Comparing to Eq. (22), we see that RH_l has been replaced by $\mathrm{RH}_s = p_v/p_v^{*,s}(T)$, which is the initial relative humidity with respect to solid (i.e., ice); c_{vl} has been replaced by c_{vs}; and E_{0v} has been replaced by $E_{0v} + E_{0s}$.

If the temperature of the LCL is below 235 K (−38°C), then there is a height between the LDL and LCL at which aqueous aerosols freeze homogeneously. As an air parcel rises up below the LCL, the aerosols absorb water so that, in equilibrium, their activity matches the liquid relative humidity. As shown by Koop et al. (2000), the homogeneous freezing temperature for aqueous aerosols is a function primarily of the activity of the aerosol solution: the temperature of homogeneous freezing for pure water (an activity of one) is 235 K (−38°C), and that temperature decreases with decreasing activity

(i.e., with decreasing liquid relative humidity). As an air parcel rises, its temperature decreases (according to the dry adiabatic lapse rate) and the activity of its aerosols increases (to match the increasing liquid relative humidity). Both of these effects bring the aerosols closer to freezing homogeneously. At a particular height, which we will refer to as the lifting freezing level (LFL), the parcel's temperature equals the homogeneous freezing temperature for the parcel's liquid relative humidity; at this level, the aerosols freeze homogeneously.

From Fig. 3 of Koop et al. (2000), we note that a 1-μm drop hits an ice supersaturation of 1.67 at 175 K. Since the homogeneous freezing of pure water occurs at −38°C (235 K) (Hoose and Möhler 2012; Koop 2015), we can parameterize the relative humidity of homogeneous freezing $\mathrm{RH}_{s,\mathrm{freeze}}$ as the following linear function of temperature:

$$\mathrm{RH}_{s,\mathrm{freeze}}(T) = \frac{p_v^{*,l}(235\,\mathrm{K})}{p_v^{*,s}(235\,\mathrm{K})} + \frac{235\,\mathrm{K} - T}{235\,\mathrm{K} - 175\,\mathrm{K}}\left[1.67 - \frac{p_v^{*,l}(235\,\mathrm{K})}{p_v^{*,s}(235\,\mathrm{K})}\right]. \tag{24}$$

At the LFL, $p_{v,\mathrm{LFL}}$ will be equal to $\mathrm{RH}_{s,\mathrm{freeze}}(T_{\mathrm{LFL}})\, p_v^{*,s}(T_{\mathrm{LFL}})$. Proceeding as in the derivation of the LDL, we get

$$T_{\mathrm{LFL}} = c\left(W_{-1}\left\{\left[\frac{\mathrm{RH}_s}{\mathrm{RH}_{s,\mathrm{freeze}}(T_{\mathrm{LFL}})}\right]^{1/a} ce^{c}\right\}\right)^{-1} T, \tag{25a}$$

$$p_{\mathrm{LFL}} = p\left(\frac{T_{\mathrm{LFL}}}{T}\right)^{c_{pm}/R_m}, \tag{25b}$$

$$z_{\mathrm{LFL}} = z + \frac{c_{pm}}{g}(T - T_{\mathrm{LFL}}), \tag{25c}$$

$$a = \frac{c_{pm}}{R_m} + \frac{c_{vs} - c_{pv}}{R_v}, \tag{25d}$$

$$b = -\frac{E_{0v} + E_{0s} - (c_{vv} - c_{vs})T_{\mathrm{trip}}}{R_v T}, \tag{25e}$$

$$c = b/a. \tag{25f}$$

Equation (25a) can be solved for T_{LFL} using a root solver. Note that, in contrast to the LCL and LDL, the approximate temperature dependence of the LFL's relative humidity makes the expression for the LFL neither exact, explicit, nor analytic.

4. Physical implications of the LCL, LDL, and LFL

For a rising air parcel, what are the physical implications of the LCL, LDL, and LFL? The LDL is the height above which the formation of an ice cloud is possible but not guaranteed. The LCL and the LFL are the heights at which an air parcel is guaranteed to become cloudy if it has not already done so.

When the temperature of the LCL is between −38° and 0°C, the rising parcel can potentially form an ice cloud anywhere between the LDL and LCL through heterogeneous deposition nucleation (i.e., the formation of ice particles by deposition of water vapor onto ice nuclei) or immersion freezing (i.e., the freezing of aqueous aerosols onto an immersed ice nuclei) (Hoose and Möhler 2012). On the other hand, in the absence of any ice nuclei, the parcel can rise up past the LCL as a supercooled liquid cloud and still not freeze until the cloud reaches the homogeneous freezing temperature of −38°C, at which point it is obligated to become an ice cloud.

When the temperature of the LCL is below −38°C, the rising parcel can potentially form an ice cloud anywhere between the LDL and LFL through heterogeneous deposition nucleation or immersion freezing. In the absence of ice nuclei, however, neither of these processes is available, and the parcel will fail to form a cloud until it gets to the LFL. At the LFL, the aqueous aerosols are forced to freeze homogeneously, and an ice cloud is born. In this way, the existence of an LFL renders the LCL irrelevant; this is the case whenever the temperature of the LCL is below −38°C.

An application of the new expressions is shown in Fig. 2, in which the LCL, LDL, and LFL are plotted as functions of surface air temperature for a surface air relative humidity (RH) of 50%. Here, we define RH as RH_s when $T < T_{\mathrm{trip}}$ and as RH_l when $T \geq T_{\mathrm{trip}}$. Also plotted on this diagram are the −38° and 0°C isotherms constructed by calculating liquid-cloud moist adiabats above the LCL. Note that the LCL curve is continued to temperatures well below −38°C; homogeneous freezing prevents the possibility of an LCL at those cold temperatures, but the LCL is plotted there to illustrate its behavior in a hypothetical world with no ice.

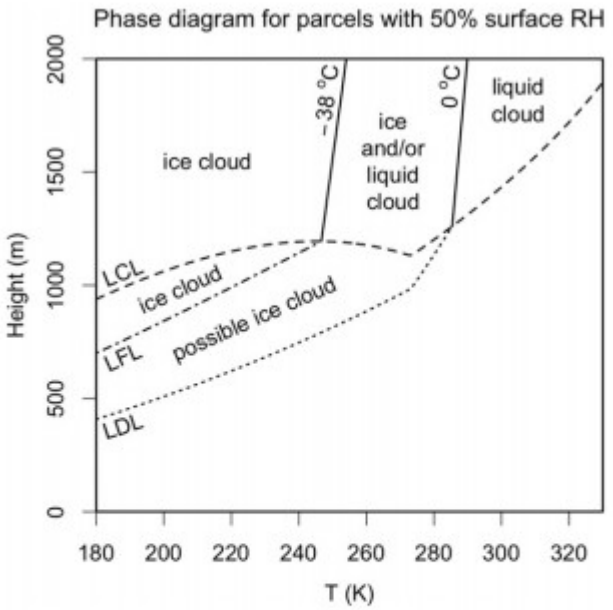

FIG. 2. For surface air with an RH of 50% with respect to liquid for $T \geq 0°$ C and with respect to solid (i.e., ice) for $T < 0°$ C, the LCL from Eq. (22) (dashed), LDL from Eq. (23) (dotted), and LFL from Eq. (25) (dash–dotted). The solid curves labeled 0° and −38°C are the parcel isotherms calculated assuming liquid-cloud moist adiabatic ascent above the LCL.

Using this diagram, we can track the evolution of an air parcel as it rises up from the surface. We can walk through three examples—corresponding to surface air temperatures of 220, 260, and 300 K—to get a feel for the behavior under conditions that demonstrate the various characteristic domains of the phase diagram.

- 220 K: A parcel that rises from the surface with a temperature of 220 K and a relative humidity of 50% hits its LDL at a height of 620 m. If there are sufficient ice nuclei for heterogeneous deposition, this parcel forms an ice cloud at or above that height. In the absence of ice nuclei, the parcel remains devoid of condensates until it reaches 990 m, which is its LFL. At this height, aerosols freeze homogeneously to form an ice cloud.
- 260 K: A parcel that rises from the surface with a temperature of 260 K and a relative humidity of 50% hits its LDL at a height of 885 m. As in the previous case, this parcel forms an ice cloud at or above its LDL if there are sufficient ice nuclei. With insufficient ice nuclei, the parcel will not nucleate any condensates until it reaches its LCL at 1180 m, at which point it forms a liquid cloud. With no ice nuclei, the parcel's condensates remain as supercooled liquid. If some ice nuclei are present, then, depending on the number concentration of ice nuclei and the elapsed time above the LCL, the parcel forms either a mixed-phase cloud or an ice cloud.
- 300 K: A parcel that rises from the surface with a temperature of 300 K and a relative humidity of 50% hits its LCL at a height of 1435 m. At the LCL, the parcel forms a liquid cloud.

5. Comparison

Figure 3a plots z_{LCL} as given by Eq. (22) for all initial temperatures from 230 to 330 K, all initial relative humidities RH_l, an initial height of zero, and an initial pressure of 1 bar. (The pressure dependence of the LCL is very weak, but the pressure is needed in order to calculate q_v, which enters into R_m and c_{pm}.) The gray region denotes where the LCL temperature would be less than 230 K, which is the lowest temperature for which we have reliable data on $p_v^{*,l}$; this is also the lowest temperature for which it makes much sense to think about an LCL since water freezes homogeneously at 235 K. Not surprisingly, at fixed temperature, the LCL lowers as the relative humidity increases. Also, at fixed relative humidity, the LCL lifts as the temperature increases. This is due to the fact that $d\log(p_v^{*,l})/dT$ is proportional to $1/T^2$: as temperature increases at fixed relative humidity, a larger temperature change (and, therefore, a larger dry adiabatic ascent) is needed to get to saturation.

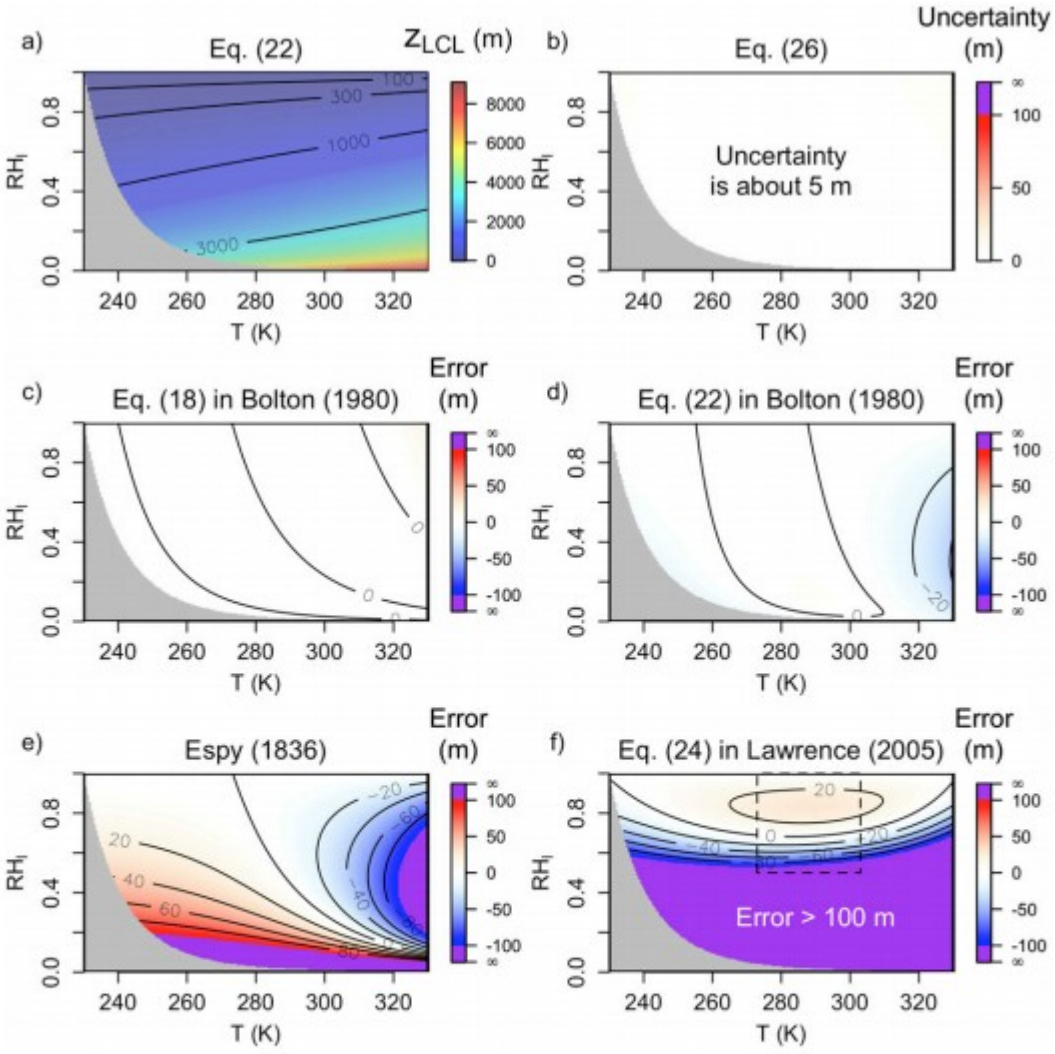

FIG. 3. (a) Contours of z_{LCL} from the exact Eq. (22) plotted for $z = 0, p = 1$ bar, for all temperatures between 230 and 330 K, and all relative humidities from 0% to 100% with respect to liquid water. The gray region marks the combinations of T and RH_l for which $T_{LCL} < 230$ K, below which we do not have empirical measurements of $p_v^{*,l}$ because of homogeneous freezing at around 235 K. (b) The uncertainties from Eq. (26). (c) The error in the numerical solution of Eq. (18) in Bolton (1980), calculated as the difference from Eq. (22). (d) As in (c), but for the analytic Eq. (22) in Bolton (1980), replicated here as Eq. (2). (e) As in (c), but for the analytic expression proposed by Espy (1836), replicated here as Eq. (1). (f) As in (c), but for Eq. (24) in Lawrence (2005), replicated here as Eq. (3). The dashed box encloses the ranges of temperature (0°–30°C) and RH (0.5–1) over which Lawrence (2005) intended for the expression to be used.

Figure 3b plots the uncertainty in the exact LCL expression due to the nonzero U given by Eq. (14). These uncertainties in the LCL are calculated as

$$\text{Uncertainty in } z_{\text{LCL}} = z_{\text{LCL}}(z, p, T, \text{RH}_l) - z_{\text{LCL}}\{z, p, T, [1 + U(T)]\text{RH}_l\} \tag{26}$$

since the fractional uncertainty in the true saturation vapor pressure translates into a fractional uncertainty in the initial RH. For all combinations

of T and RH in the ranges considered, this error in the predicted LCL lies in the range of 4–6 m (i.e., the uncertainty is about 5 m).

The remaining panels of Fig. 3 plot the errors in the previous approximations to the LCL, calculated as the difference between their prediction for the LCL and the actual value from Eq. (22). Figure 3c plots the error in Eq. (18) of Bolton (1980), which is solved using a numerical root finder. Over all possible LCLs, its maximum error is 20 m, which occurs at the highest temperatures and relative humidities in Fig. 3c; this maximum error exceeds the uncertainty of 5 m. Figure 3d plots the error in Eq. (22) of Bolton (1980), which is printed here in Eq. (2). Its maximum error is 40 m. Figure 3e plots the error in the equation of Espy (1836) as subsequently modified and printed here in Eq. (1). Its maximum error is 665 m. Finally, Fig. 3f plots the error in the Eq. (24) of Lawrence (2005), which is printed here in Eq. (3). Its maximum error is 7130 m. The dashed box encloses the ranges of temperature (0°–30°C) and relative humidity (0.5–1) over which Lawrence (2005) intended for the expression to be used; in those ranges of temperature and humidity, the maximum error is 170 m.

Figure 4a plots the LDL given by the exact analytic Eq. (23) for all temperatures from 180 to 273 K, all relative humidities RH_s, and a pressure of 1 bar. The gray region denotes where the LDL temperature would be less than 180 K, which is the lowest temperature for which we have reliable data on $p_v^{*,s}$. Figure 3b plots the uncertainty in the exact LDL expression due to the nonzero U given by Eq. (14). As for the LCL, the uncertainties in the LDL are calculated as

$$\text{Uncertainty in } z_{\mathrm{LDL}} = z_{\mathrm{LDL}}(z,p,T,\mathrm{RH}_s) - z_{\mathrm{LDL}}\{z,p,T,[1+U(T)]\mathrm{RH}_s\}. \quad (27)$$

For all possible LDLs, the uncertainties lie in the range of 4–6 m (i.e., the uncertainty is about 5 m).

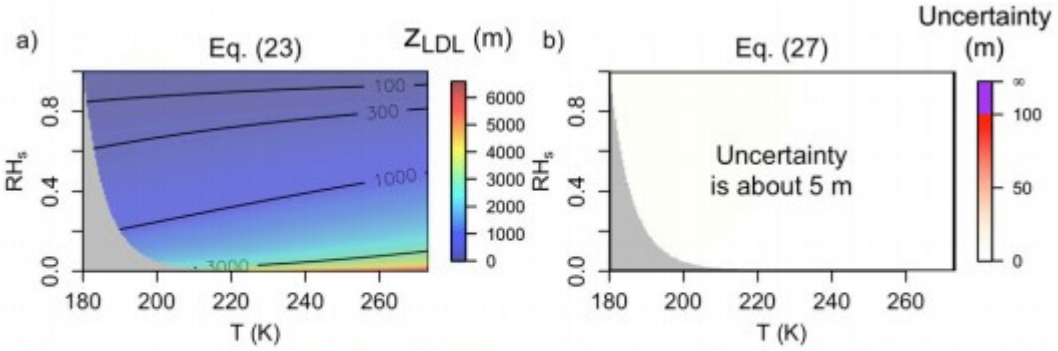

FIG. 4. (a) Contours of z_{LDL} from the exact Eq. (23) plotted for $z = 0, p = 1$ bar, for all temperatures between 180 and 273 K, and all surface relative humidities from 0% to 100% with respect to solid water. The gray region marks the combinations of T and RH_s for which $T_{\mathrm{LDL}} < 180$ K, below which we do not have empirical measurements of $p_v^{*,s}$. (b) The uncertainties from Eq. (27).

6. The ice-supersaturated layer

Figure 5a plots the LCL minus the LDL as a function of temperature T and relative humidity with respect to ice RH_s. This serves as an upper bound on the thickness of the ice-supersaturated layer underneath the liquid cloud base. As discussed in section 4, the LCL is irrelevant when its temperature is below about −38°C. At those temperatures, the LFL lies below the LCL, so rising parcels will form ice clouds before they reach the LCL. Therefore, the depth of the potentially ice-supersaturated layer is $\min(z_{\mathrm{LCL}}, z_{\mathrm{LFL}}) - z_{\mathrm{LDL}}$. This is plotted in Fig. 5b, where we see that the maximum depth of the supersaturated layer is about 400 m. We can summarize Fig. 5b as follows. For any surface air temperature, there is a sufficiently low relative humidity (i.e., a relative humidity below the 0°C LCL isotherm in Fig. 5b) that, in the absence of ice nuclei, will generate an ice-supersaturated layer just below the cloud base. For surface air temperatures below 0°C, a subcloud ice-supersaturated layer is a possibility for all surface air relative humidities. The maximum depth of that layer occurs when the LCL has a temperature of −38°C; at this temperature, the depth of the ice-supersaturated layer is about 400 m. For colder LCLs, the depth of the supersaturated layer decreases to about 300 m at the coldest surface air temperatures observed on Earth.

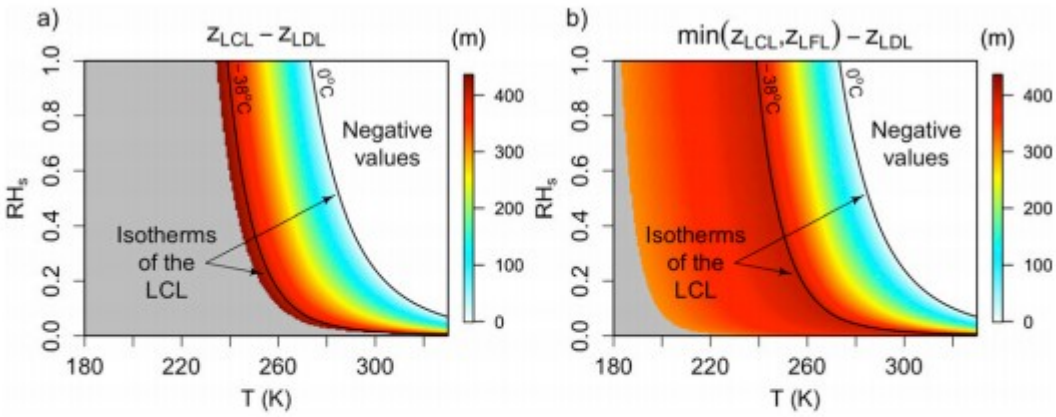

FIG. 5. (a) Plot of z_{LCL} minus z_{LDL} as a function of surface air temperature and surface air relative humidity with respect to ice. Negative values are not plotted because they are not of interest (if the LCL is lower than the LDL, then the LDL is irrelevant). The two contours denote the 0° and −38°C isotherms of the LCL. The gray region marks the combinations of T and RH_s for which $T_{\mathrm{LCL}} < 230\,\mathrm{K}$. (b) As in (a), but for $\min(z_{\mathrm{LCL}}, z_{\mathrm{LFL}})$ minus z_{LDL}, where the LFL is the level of homogeneous freezing of aerosols. The gray region marks the combinations of T and RH_s for which $T_{\mathrm{LFL}} < 180\,\mathrm{K}$.

7. Summary

Expressions for the lifting condensation level (LCL) and the lifting deposition level (LDL) have been derived that are exact, explicit, and analytic; they are given in Eqs. (22) and (23). These expressions are given in terms of fundamental constants, which may be adapted to extraterrestrial atmospheres with a condensible gas that can be adequately described with constant heat capacities. An expression is also given for the lifting freezing

level (LFL), defined as the height at which aqueous aerosols freeze homogeneously. That expression, given in Eq. (25), depends on an approximate equation for the homogeneous freezing activity; this makes the expression implicit, thereby requiring a numerical root solver for evaluation. These expressions then allow for a quantification of the maximum thickness of ice-supersaturated layers underlying liquid cloud–topped boundary layers. On Earth, the maximum potential thickness is about 400 m, which can be attained when the LCL is at the homogeneous freezing temperature of 235 K.

Acknowledgments

This work was supported primarily by the U.S. Department of Energy's (DOE) Atmospheric System Research, an Office of Science, Office of Biological and Environmental Research program; Lawrence Berkeley National Laboratory is operated for the DOE by the University of California under Contract DE-AC02-05CH11231. The author is grateful to Alan Betts, Ronald Cohen, Mark Lawrence, and an anonymous reviewer for their helpful feedback.

REFERENCES

Atreya, S. K., E. Y. Adams, H. B. Niemann, J. E. Demick-Montelara, T. C. Owen, M. Fulchignoni, F.Ferri, and E. H. Wilson, 2006: Titan's methane cycle. *Planet. Space Sci.*, 54, 1177–1187, doi:https://doi.org/10.1016/j.pss.2006.05.028.

Bielska, K., D. K. Havey, G. E. Scace, D. Lisak, A. H. Harvey, and J. T. Hodges, 2013: High-accuracy measurements of the vapor pressure of ice referenced to the triple point. *Geophys. Res. Lett.*, 40, 6303–6307, https://doi.org/https://doi.org/10.1002/2013GL058474.

Bolton, D., 1980: The computation of equivalent potential temperature. *Mon. Wea. Rev.*, 108, 1046–1053, doi:https://doi.org/10.1175/1520-0493(1980)108<1046:TCOEPT>2.0.CO;2.

Brasseur, G. P., and D. J. Jacob, 2017: *Modeling of Atmospheric Chemistry.* 1st ed. Cambridge University Press, 632 pp.

Cotton, W. R., G. Bryan, and S. C. Van den Heever, 2011: *Storm and Cloud Dynamics.* 2nd ed. International Geophysics Series, Vol. 99, Academic Press, 820 pp.

Davis, W. M., 1889: Some American contributions to meteorology. *J. Franklin Inst.*, 127, 176–191, doi:https://doi.org/10.1016/0016-0032(89)90145-2.

Emanuel, K. A., and M. Živković-Rothman, 1999: Development and evaluation of a convection scheme for use in climate models. *J. Atmos. Sci.*, 56, 1766–1782, doi:https://doi.org/10.1175/1520-0469(1999)056<1766:DAEOAC>2.0.CO;2.

Espy, J. P., 1836: Essays on meteorology. No. IV: North east storms, volcanoes, and columnar clouds. *J. Franklin Inst.*, 22, 239–246, doi:https://doi.org/10.1016/S0016-0032(36)91215-2.

Hoose, C., and O. Möhler, 2012: Heterogeneous ice nucleation on atmospheric aerosols: A review of results from laboratory experiments. *Atmos. Chem. Phys.*, 12, 9817–9854, doi:https://doi.org/10.5194/acp-12-9817-2012.

Koop, T., 2015: Atmospheric water. *Proc. Int. School of Physics "Enrico Fermi,"* Varenna, Italy, Società Italiana di Fisica, 45–75.

Koop, T., B. Luo, A. Tsias, and T. Peter, 2000: Water activity as the determinant for homogeneous ice nucleation in aqueous solutions. *Nature*, 406, 611–614, doi:https://doi.org/10.1038/35020537.

Lawrence, M. G., 2005: The relationship between relative humidity and the dewpoint temperature in moist air: A simple conversion and applications. *Bull. Amer. Meteor. Soc.*, 86, 225–233, doi:https://doi.org/10.1175/BAMS-86-2-225.

McDonald, J. H., 1963: James Espy and the beginnings of cloud thermodynamics. *Bull. Amer. Meteor. Soc.*, 44, 634–641.

Murphy, D. M., and T. Koop, 2005: Review of the vapour pressures of ice and supercooled water for atmospheric applications. *Quart. J. Roy. Meteor. Soc.*, 131, 1539–1565, doi:https://doi.org/10.1256/qj.04.94.

Nelder, J. A., and R. Mead, 1965: A simplex method for function minimization. *Comput. J.*, 7, 308–313, doi:https://doi.org/10.1093/comjnl/7.4.308.

Riegel, C. A., 1992: *Fundamentals of Atmospheric Dynamics and Thermodynamics.* 1st ed. World Scientific, 496 pp.

Romps, D. M., 2008: The dry-entropy budget of a moist atmosphere. *J. Atmos. Sci.*, 65, 3779–3799, doi:https://doi.org/10.1175/2008JAS2679.1.

Romps, D. M., 2015: MSE minus CAPE is the true conserved variable for an adiabatically lifted parcel. *J. Atmos. Sci.*, 72, 3639–3646, doi:https://doi.org/10.1175/JAS-D-15-0054.1.

Romps, D. M., and Z. Kuang, 2010: Do undiluted convective plumes exist in the upper tropical troposphere? *J. Atmos. Sci.*, 67, 468–484, doi:https://doi.org/10.1175/2009JAS3184.1.

Sonntag, D., 1990: Important new values of the physical constants of 1986, vapour pressure formulations based on the ITS-90, and psychrometer formulae. *Z. Meteor.*, 70, 340–344.

Sonntag, D., and D. Heinze, 1982: *Sättigungsdampfdruck und Sättigungsdampfdichtetafeln für Wasser und Eis.* Verlag, 54 pp.

Tsonis, A. A., 2002: *An Introduction to Atmospheric Thermodynamics.* 1st ed. Cambridge University Press, 171 pp.

Wagner, W., and A. Pruß, 2002: The IAPWS formulation 1995 for the thermodynamic properties of ordinary water substance for general and

scientific use. *J. Phys. Chem. Ref. Data*, 31, 387–535, doi:https://doi.org/10.1063/1.1461829.

Wagner, W., T. Riethmann, R. Feistel, and A. H. Harvey, 2011: New equations for the sublimation pressure and melting pressure of H2O ice Ih. *J. Phys. Chem. Ref. Data*, 40, 043103, https://doi.org/https://doi.org/10.1063/1.3657937.

Wallace, J. M., and P. V. Hobbs, 2006: *Atmospheric Science: An Introductory Survey.* 2nd ed. Elsevier, 504 pp.

Wetzel, P. J., 1990: A simple parcel method for prediction of cumulus onset and area-averaged cloud amount over heterogeneous land surfaces. *J. Appl. Meteor.*, 29, 516–523, doi:https://doi.org/10.1175/1520-0450(1990)029<0516:ASPMFP>2.0.CO;2.

APPENDIX

Empirical Saturation Vapor Pressure

In Fig. 1a, the equations for saturation vapor pressure over solid water $p_v^{*,s}$ from Sonntag (1990), Murphy and Koop (2005), and Wagner et al. (2011) are as follows. The equation from Sonntag (1990) is

$$p_v^{*,s} = 100 \exp[24.7219 - 6024.5282 T^{-1} + 0.010\,613\,868 T - 0.000\,013\,198\,825 T^2 - 0.493\,825\,77 \log(T)], \quad \text{(A1)}$$

where T is in kelvins and $p_v^{*,s}$ is in pascals. The equation from Murphy and Koop (2005) is

$$p_v^{*,s} = \exp[9.550\,426 - 5723.265 T^{-1} + 3.530\,68 \log(T) - 0.007\,283\,32 T], \quad \text{(A2)}$$

where T is in kelvins and $p_v^{*,s}$ is in pascals. The equation from Wagner et al. (2011) is

$$p_v^{*,s} = p_t \exp[\theta^{-1}(a_1 \theta^{b_1} + a_2 \theta^{b_2} + a_3 \theta^{b_3})], \quad \text{(A3)}$$

where $p_t = 611.6573\,\text{Pa}$, $\theta = T/T_t$, $T_t = 273.16\,\text{K}$, $a_1 = -0.212\,144\,006 \times 10^2$, $a_2 = 0.273\,203\,819 \times 10^2$, $a_3 = -0.610\,598\,130 \times 10^1$, $b_1 = 0.333\,333\,333 \times 10^{-2}$, $b_2 = 0.120\,666\,667 \times 10^1$, and $b_3 = 0.170\,333\,333 \times 10^1$.

In Fig. 1b, the equations for saturation vapor pressure over liquid water $p_v^{*,l}$ from Sonntag and Heinze (1982), Murphy and Koop (2005), and Wagner and Pruß (2002) are as follows. The equation from Sonntag and Heinze (1982) is

$$p_v^{*,l} = \exp[21.124\,995\,2 - 6094.4642 T^{-1} - 0.027\,245\,552 T + 0.000\,016\,853\,396 T^2 + 2.457\,550\,6 \log(T)], \quad \text{(A4)}$$

where T is in kelvins and $p_v^{*,l}$ is in pascals. The equation from Murphy and Koop (2005) is

$$p_v^{*,l} = \exp\{54.842\,763 - 6763.22T^{-1} - 4.210\log(T) + 0.000\,367T + \tanh[0.0415(T - 218.8)][53.878 - 1331.22T^{-1} - 9.445\,23\log(T) + 0.014\,025T]\}, \quad \text{(A5)}$$

where T is in kelvins and $p_v^{*,l}$ is in pascals. The equation from Wagner and Pruß (2002) is

$$p_v^{*,l} = p_c \exp\left[\frac{T_c}{T}(a_1\theta + a_2\theta^{1.5} + a_3\theta^3 + a_4\theta^{3.5} + a_5\theta^4 + a_6\theta^{7.5})\right], \quad \text{(A6)}$$

where $\theta = 1 - T/T_c$, $T_c = 647.096\,\text{K}$, $p_c = 22.064 \times 10^6\,\text{Pa}$, $a_1 = -7.859\,517\,83$, $a_2 = 1.844\,082\,59$, $a_3 = -11.786\,649\,7$, $a_4 = 22.680\,741\,1$, $a_5 = -15.961\,871\,9$, and $a_6 = 1.801\,225\,02$.